

# Performance of LDPC- Coded APSK-Modulation for Wireless USB

C.T.MANIMEGALAI<sup>1</sup>, R.KUMAR<sup>2</sup>  
 Dept of Electronics and Communication  
 SRM University,  
 Kattankulathur (T.N)-INDIA

*Abstract* – The creation of Ultra-Wideband (UWB) radio platform has allowed the development of high bit-rate Wireless-USB offering High Definition video streaming. Quadrature Phase Shift Keying (QPSK) and Dual Carrier Modulation (DCM) are the current modulation schemes used for Multiband Orthogonal Frequency Division Multiplexing (MB-OFDM) in the ECMA-368 defined UWB radio platform. ECMA-368 offers up to 480 Mb/s instantaneous bit rate to the Medium Access Control (MAC) layer to enable the high-rate transmission, but depending on radio channel conditions dropped packets unfortunately result in a lower throughput. This paper presents a higher data rate Coded modulation scheme that fits within the configuration of the current standard to increase the system throughput by achieving 960 Mb/s (reliable to 3 meters) thus maintaining the high rate USB throughput even with a moderate level of dropped packets. The system performance for LDPC coded 32-APSK modulation is simulated in realistic multipath environments.

*Keywords:* APSK (Amplitude Phase Shift Key), Multi band-Orthogonal frequency-division multiplexing (MB-OFDM), ultra-wideband (UWB), wireless personal area networks (WPAN).

## 1 Introduction

UWB systems were recently proposed to standardize wide bandwidth wireless communication systems, particularly for Wireless Personal Area Networks (WPAN). The fundamental issue of UWB is that the transmitted signal can be spread over an extremely large bandwidth with a very low Power Spectral Density (PSD). In 2005 the WiMedia Alliance [19] working with the European Computer Manufacturers Association (ECMA) announced the establishment of the WiMedia MB-OFDM (Multiband Orthogonal Frequency Division Multiplexing) UWB radio platform as their global UWB standard, ECMA-368 [18] and the latest updated version [17] incorporating spectral nulling. ECMA-368 was also chosen as Physical layer (PHY) of high data rate wireless specifications for high-speed Wireless USB (W-USB) [16].

Quadrature Phase Shift Keying (QPSK) and Dual Carrier Modulation (DCM) are exploited as standard modulation schemes for MB-OFDM in ECMA-368. QPSK constellation is used for data rates 200 Mb/s and lower while DCM is used as a multi-dimensional constellation for data rates 320 Mb/s and higher.

However the maximum data rate of 480 Mb/s in a practical environment can not be achieved due to poor radio channel conditions causing dropped packets, resulting in a lower throughput and the need to retransmit the dropped packets. To increase the bit rate and allow for effective 480 Mb/s performance even with moderate packet loss in a practical system, rectangular Gray coded 16-QAM can be employed. However the system using the 16-QAM has no successful multipath propagation link for transmitting at 960 Mb/s or only achieves approximately 1 meter at 640 Mb/s comparing to the DCM 480 Mb/s mode and 320 Mb/s mode respectively (Appendix A). In this paper, a low power and high performance LDPC –Coded APSK-modulation scheme is proposed, implemented and tested in fixed point model, which increases the MB-OFDM system throughput to 960 Mb/s (comparing to the DCM 480 Mb/s mode) with a successful link of 3 meters. UWB communication systems use signals with a bandwidth that is larger than 25% of the center frequency or more than 500MHz. the UWB communications transmit in a way that doesn't interfere largely with other more traditional narrow-band and continuous carrier wave uses in the same frequency band

In this paper, an enhancement to the UWB system was proposed, where the QPSK DCM and QAM was

replaced by APSK modulation technique which provides better throughput with optimum power and distortion.

Chapter 2 presents the MB-OFDM background. Chapter 3 describes about the system model .Chapter 4 describes about the LDPC coding system .Chapter 5 describes about the APSK constellation design. Chapter 6 describes about the Log likelihood ratio detection method. Chapter 7describes about the Data rate Vs maximum distance. Chapter 8 describes about the Channel Capacity Chapter. 9describes about the Maximum power transfer Chapter .10describes about the Proposed system. Chapter 11describes about the Conclusion.

## 2 MB-OFDM IN ECMA-368

The ECMA-368 specifies an MB-OFDM system occupying 14 bands with a bandwidth of 528 MHz for each band. The first 12 bands are grouped into 4 band groups (BG1-BG4), and the last two bands are grouped into a fifth band group (BG5). A sixth band group (BG6) containing band 9, 10 and 11 is also defined within the spectrum of BG3 and BG4, in agreement to usage within worldwide spectrum regulations. The advantage of the grouping is that the transmitter and receiver can process a smaller bandwidth signal while taking advantages from frequency hopping. At the heart of ECMA-368 lies a 128-pt IFFT resulting in each IFFT sub-carrier being clocked at 528MHz. The subcarriers in each OFDM symbol include 100 data subcarriers, 12 pilot subcarriers, 6 NULL valued subcarriers and 10 guard subcarriers. The 10 guard subcarriers used for mitigating Inter Symbol Interference (ISI) are located on either edge of the OFDM symbol and have same value as the 5 outermost data subcarriers. In addition, the guard carriers can be used as another form of time and frequency diversity resulting in improving receiver performance [15][14]. Each OFDM symbol is separated with a Zero Padded Suffix (ZPS) of 70.08ns to aid multipath interference mitigation and settling times of the transmitter and receiver .

## 3 SYSTEM MODEL

The multiband-OFDM (MB-OFDM) approach[5],[6], the available UWB spectrum is divided into several sub-bands of smaller bandwidth. An OFDM symbol is transmitted in each sub-band and then, the system switches to another sub-band. Amplitude phase-shift keying(PSK)modulation is used for OFDM. The transmitted signal in this is given by[10].

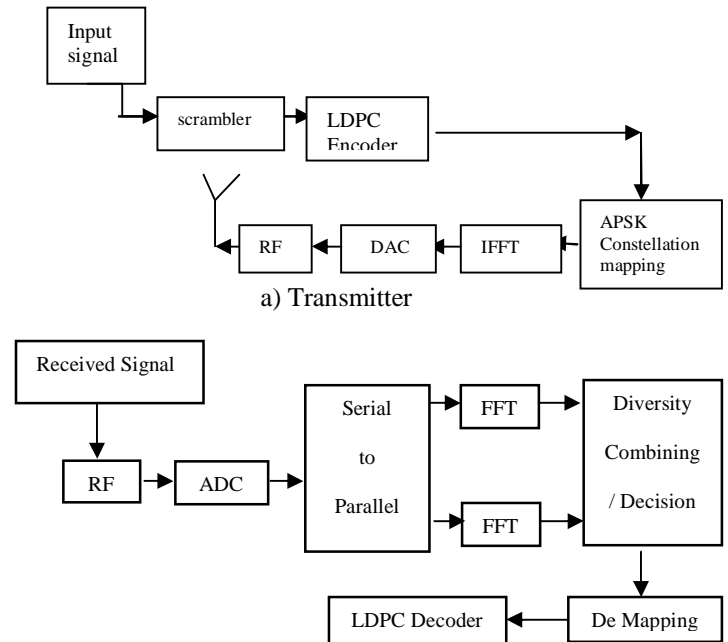


Fig. 1 Ultrawideband OFDM transceiver

## 4 LOW-DENSITY PARITY-CHECK CODE

In information theory, a low-density parity-check (LDPC) code is a linear error correcting code, a method of transmitting a message over a noisy transmission channel, and is constructed using a sparse bipartite graph. LDPC codes are capacity-approaching codes, which means that practical constructions exist that allow the noise threshold to be set very close (or even arbitrarily close on the BEC) to the theoretical maximum (the Shannon limit) for a symmetric memory-less channel. The noise threshold defines an upper bound for the channel noise, up to which the probability of lost information can be made as small as desired. Using iterative belief propagation techniques, LDPC codes can be decoded in time linear to their block length[13].

LDPC codes are finding increasing use in applications requiring reliable and highly efficient information transfer over bandwidth or return channel-constrained links in the presence of data-corrupting noise. Although implementation of LDPC codes has lagged behind that of other codes, notably turbo codes, the absence of encumbering software patents has made LDPC attractive to some. LDPC codes are also known as Gallager codes, in honor of Robert G. Gallager, who developed the LDPC

concept in his doctoral dissertation at MIT in 1960[12].

### 5 APSK CONSTELLATION DESIGN

In this section, we define the generic multiple-ring APSK constellation family of 16, 32, and 64 digital constellations points. [2]

#### 5.1 APSK Constellation

An M-APSK Constellation is composed of R concentric rings, each with uniformly spaced PSK points. The M-APSK constellation set x is given by [1]

$$x = \begin{cases} r_1 \exp\left(j\left(\frac{2\pi}{n_1}i + \theta_1\right)\right) & i = 0, \dots, n_1 - 1 \\ r_2 \exp\left(j\left(\frac{2\pi}{n_2}i + \theta_2\right)\right) & i = 0, \dots, n_2 - 1 \\ \vdots \\ r_R \exp\left(j\left(\frac{2\pi}{n_R}i + \theta_R\right)\right) & i = 0, \dots, n_R - 1 \end{cases} \quad (1)$$

Where  $n_l$ ,  $r_l$  and  $\theta_l$  ( $l=1, \dots, R$ ) denote the number of points, the radius and the phase offset of the  $l$ -th ring respectively, In [11], a general M-APSK construction strategy was introduced, which includes 3 steps:

- i) Selecting R and  $n_l$
- ii) Determining  $r_l$ , and
- iii) Choosing  $\theta_l$ .

Such modulation schemes are termed hereinafter as  $n_1 + n_2 + \dots + n_{nR}$  - APSK.

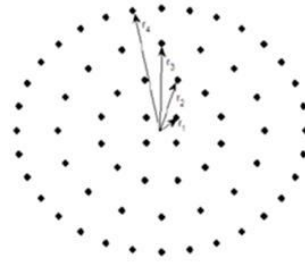
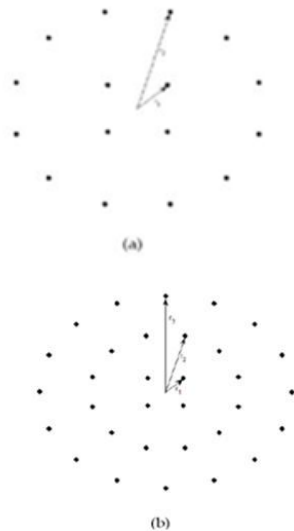


Fig. 3 (a) 4+12-APSK, 3 (b) 4+12+16-APSK and 3 (c) 4+12+16+32-APSK constellations

Table 1 shows the optimized M-APSK parameters for various coding rates r giving an optimum constellation for each given spectral efficiency R.

Numerical results for 16-APSK [3]

MODULATION ORDER	CODING RATE R	SPECTRAL EFFICIENCY R (BPS/Hz)	P <sub>2</sub> <sup>OPT</sup>
4+12 APSK	2/3	2.67	3.15
	3/4	3.00	2.85
	4/5	3.20	2.75
	5/6	3.33	2.70
	8/9	3.56	2.60
	9/10	3.60	2.57

Numerical results for 32-APSK

MODULATION ORDER	CODING RATE R	SPECTRAL EFFICIENCY R (BPS/Hz)	P <sub>2</sub> <sup>OPT</sup>	P <sub>3</sub> <sup>OPT</sup>
4+12+16 APSK	3/4	3.75	2.84	5.27
	4/5	4.00	2.72	4.87
	5/6	4.17	2.64	4.64
	8/9	4.44	2.54	4.33
	9/10	4.50	2.53	4.30

Numerical results for 64-APSK

MODULATION ORDER	CODING RATE R	SPECTRAL EFFICIENCY R (BPS/Hz)	P <sub>1</sub> <sup>OPT</sup>	P <sub>2</sub> <sup>OPT</sup>	P <sub>3</sub> <sup>OPT</sup>	P <sub>4</sub> <sup>OPT</sup>
4+12+16+32 APSK	0.818	4.91	0.051	0.028	0.019	0.0049
	0.858	5.15	0.047	0.025	0.019	0.0065
	0.905	5.43	0.040	0.022	0.018	0.0090

#### 5.2 SER for APSK Modulation

The union bound the symbol error rate (SER) of M-ary modulation is given as

$$p(E) = \frac{1}{M} \sum_{i=1}^M p(E|S_i) \leq \sum_{j=1, j \neq i}^M p(S_i \rightarrow S_j) \quad (2)$$

Where E denotes the error event and  $p(S_i \rightarrow S_j)$  denotes the pairwise probability that transmitted symbol  $S_i$  is erroneously detected to  $S_j$ . Using the erfc-function and the Euclidean distance  $d_{i,j}$  between symbols  $S_i$  and  $S_j$ , Pair Wise error probability  $p(S_i \rightarrow S_j)$  is determined as

$$p(S_i \rightarrow S_j) = \frac{1}{2} \operatorname{erfc} \left( \sqrt{\frac{d_{i,j}^2}{4N_0}} \right) \quad (3)$$

Where  $N_0$  is the single-sided noise spectral density. For MAPSK constellation, the SER of MAPSK modulation can be written as by means of symmetry in the constellation:

$$p_{MAPSK}(E) = \frac{1}{M} \sum_{k=0}^n p(E|S_k) \leq \frac{1}{M} \sum_{k=0}^n \sum_{k=0}^n \left( \frac{1}{2} \operatorname{erfc} \left( \sqrt{\frac{d_{i,j}^2}{4N_0}} \right) \right) \quad (4)$$

According to the circular characteristics of MAPSK constellation, the Euclidean distance  $d_{ij}$  can be divided into two parts: intra-ring distance  $d_{(intra)}$  and inter-ring distance  $d_{(inter)}$

$$d_{i(intra)} = 2 \cdot r_i^2 \sin \left( \frac{\pi}{n_i} \right) \quad (5)$$

$$d_{i,i+1(inter)} = r_i^2 + r_{i+1}^2 - 2r_i r_{i+1} \cos(\theta_{i,i+1}) \quad (6)$$

Where  $n_i$  is the number of possible alphabets on  $i$ th ring  $\theta_{i,i+1}$  is the relative phase between  $i$ th ring and  $i + 1$ th ring. which can be achieved through the geometry characteristics[4]-[6].

The equation (4) can be written as:

$$p_{MAPSK}(E) = \frac{1}{M} \sum_{k=0}^n p(E|S_k) \leq \sum_{k=0}^i \frac{n_k}{M} \cdot \frac{1}{2} \operatorname{erfc} \left( \sqrt{\frac{d_{i(intra)}^2}{4N_0}} \right) + \sum_{i=0}^i \frac{n_i}{M} \cdot \frac{1}{2} \operatorname{erfc} \left( \sqrt{\frac{d_{i,i+1(inter)}^2}{4N_0}} \right) \quad (7)$$

## 6 LOG LIKELIHOOD RATIO

Soft decision decoders take as input the log likelihood ratio(LLR) for each code bit [5]. Suppose

its  $b = b_{m-1} b_{m-2} \dots b_0$  are mapped to the complex constellation point  $c = c(b)$ . Let  $r = c + n$  denote the noisy received symbol[15]-[17].

### 6.1 LLR for 16-APSK

The four bit LLRs for each 16-APSK symbol can be computed using [7]-[9]

$$\lambda_j = \ln \left[ \frac{\sum_{b:bj=0} \exp \left( \frac{\langle r, c(b) \rangle}{\sigma^2} \right)}{\sum_{b:bj=1} \exp \left( \frac{\langle r, c(b) \rangle}{\sigma^2} \right)} \right] \quad (8),$$

with eight terms each in the numerator and denominator. As there is no apparent simplification of this exact LLR expression, the approximate LLR computation of

$$\lambda_j \approx \frac{\langle r, c^*(j,0) - c^*(j,1) \rangle}{\sigma^2} \quad (9)$$

can be used when a lower complexity computation is needed.

To identify the closest constellation point with a 0 or a 1 in the bit position of interest, one could compute the distances to all sixteen constellation points. As was the case for 8-PSK, this is unnecessary. Since 16-APSK is simply the union of two PSK modulations, the angle comparison approach used for 8-PSK can be used to identify the closest inner-ring constellation point with a 0 in the bit position of interest, and separately, to identify the closest outer-ring constellation point. Then can be computed for each of the two candidate constellation points to find the closer point. This requires computation of a total of four inner products, or eight multiplications, to compute an approximate bit LLR.

### 6.2 LLR for 32-APSK

The five bit LLRs for each 32-APSK symbol can be computed using

$$c^*(j,i) \Delta_c \left( \underset{b:bj=i}{\operatorname{argmin}} \|r - c(b)\|^2 \right) \quad (10),$$

with sixteen terms each in the numerator and denominator. As there is no apparent simplification of this exact LLR expression, the approximate LLR computation of

$$\lambda_j \approx \frac{\langle r, c^*(j,0) - c^*(j,1) \rangle}{\sigma^2} \quad (11)$$

can be used when a lower complexity computation is needed. Since 32-APSK is the union of three PSK modulations, the angle comparison approach used for 8-PSK can be used to identify the closest constellation point with a 0 in the bit position of interest, on each ring. Then,  $\lambda_j$  can be computed for each of the three candidate constellation points to find the closest point. The same type of calculation is made for constellation points with a 1 in the bit position of interest. This requires computation of a total of six inner products, or twelve multiplications, to compute an approximate bit LLR. The Voronoi boundaries of 32-APSK are not all horizontal, vertical, or at a 45 degree angle, so the more efficient method detailed above for 16-APSK could not be used for 32-APSK.

## 7 Data rate and maximum distance

For simplicity, let us suppose that the signal propagation occurs over a free-space. Thus the free-space attenuation  $A_m$  is expressed by: [1-4]

$$A_m(f) = \frac{(4\pi)^2 D^2 f^2 L}{G_T G_R C^2} \quad (20)$$

Where  $D$  is distance of propagation,  $G_T G_R$  are transmitter and receiver antenna gain,  $f$  is operation frequency and  $C$  is speed of light. For our simulations,  $L=1$ , which indicates no loss in the system hardware. Suppose now the transmitted waveform is characterized by  $P_s = \int_{f_L}^{f_H} P_t(f) df$ . In our example, the pulse waveform is the 5th derivative of a monocyclic Gaussian pulse, and its PSD given by:

$$P_s(f) = A_{\max} \frac{(2\pi f \delta)^{2n} e^{-(2\pi f \delta)^2}}{n^n e^{-n}}; \quad (12)$$

$$A_m = 10^{-13.125}; \delta = 51 ps$$

$A_m$  and  $\delta$  are normalized pulse parameters that make the PSD of transmitted power match FCC indoor emission mask. We can express the receiver signal power as:

$$P_r = \int_{f_L}^{f_H} |H(f)|^2 P_t(f) df$$

$$P_r = \frac{M_s SNR_{spec} N_o}{2}$$

$$P_r = \frac{M_s SNR_{spec} N_o}{2}; N_o = K T_o F_{sys} \quad (13)$$

Where

$$F_{sys} = \frac{T_{ant}}{T_o} + F_1 + \frac{F_2 - 1}{G_1} + \frac{F_3 - 1}{G_1 G_2} + \dots, H(f)$$

is frequency response of the indoor channel that we mentioned, and can be expressed as:

$$|H(f)| = \sqrt{\frac{1}{A_m(f)} R(f)} \quad (14)$$

Where  $R(f)$  is the shadowing parameter that depends on the geography of propagation (6dB),  $T_o$  is noise temperature on the receiver antenna,  $F_1$  and  $F_2$ , are receiver component noise factors,  $G_1$  and  $G_2$  are the gains of receiver system components and  $M_s$  is system margin (1 dB). By substituting E(14) into E(15) we get [4]:

$$D^2 \frac{G_T G_R c^2}{(4\pi)^2 R_b} \frac{2 \int_{f_L}^{f_H} \frac{P_s(f)}{f^2} df}{M_s SNR_{spec} \frac{1}{2} F_{sys} k T_o} \quad (15)$$

Where  $R_b$  is data rate. Given SNR(spec) which corresponds to the SER of a specific modulation scheme, we can evaluate the maximum distance. Fig (4) shows, the maximum distance as an function of data rate in APSK, QPSK and QAM modulation schemes. It is observed that 32-APSK has the best data rate over short distances; Fig(4) shows at large distances, modulation schemes suffer from decreased data rates.

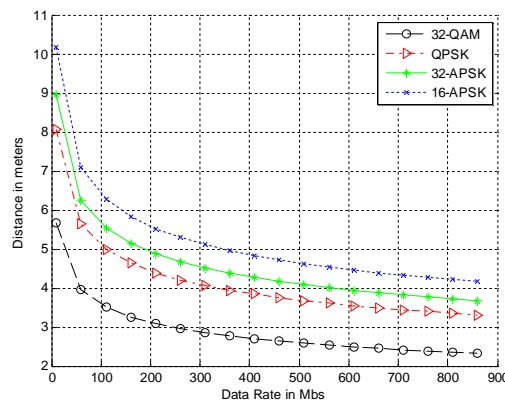


Fig.4 Comparison of modulation schemes with distance

### 8 Channel capacity

A method for calculating the channel capacity for M-ary digital modulation signal set over an AWGN channel is evaluated. The Shannon capacity given by Equation below

$$C = W \log_2(1 + S^T Q_c^{-1} S) = \frac{1}{2} \log_2(1 + SNR) \quad (16)$$

Where W is channel band-width, predicts the channel capacity with continuous value input-output. Fig(5) shows UWB capacity, compared to other unlicensed systems, such as ISM(2.4-2.483GHZ) andUN1(5.15-5.25GHZ).It is illustrated UWB has a highest capacity over short distances[7].

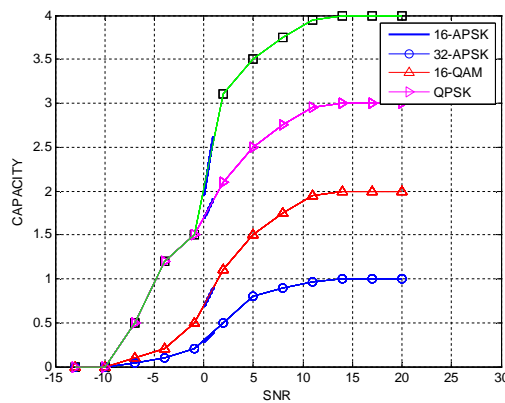


Fig.5 Capacity Analysis of different modulation schemes Modulation

### 9 Maximum transfer Power

From a communications theory perspective, perhaps the most important characteristic of UWB systems is power-limited regime operation. The FCC specifies a limit on the maximum power that UWB devices may transmit, which is given in T(7).

T(7)FCC limitation[1]:

$$\begin{aligned}
 P_{M \max} &= \int_{f_l}^{f_h} P(f)df; f_h = 3.1GHz, f_l = 10.6GHz \\
 P_{M \max}(db) &= 10\log_{10}\left(\int_{f_l}^{f_h} P(f)df; f_h\right); \\
 &= -41.3 + 10\log_{10}(7.5 \cdot 10^3 / 1) = 0.55mW = -2.8dbm, PSD < -41.3^{dbm} / MHz \\
 fractional_{BW} &= \frac{(f_H - f_L)}{\left[\frac{f_H + f_L}{2}\right]} \geq 0.2 \text{ or } S_{BW} \geq 500MHz \quad (17)
 \end{aligned}$$

The maximum legal transmitter power, Pt, can be found and will affect the maximum transmit distance and data rate. In this case, the upper bound will be -

5dB(total transmitted power over channel bandwidth),

$$\frac{P_t}{P_r}(dB) = C_0 + 10n \log_{10}\left[\frac{\lambda}{4\pi d}\right] + X_R(dB) \quad (18)$$

$$P_t \geq \frac{M_z R_b E_b^0}{G_T G_R} \left[\frac{4\pi}{\lambda}\right]^2 d^2(W) \quad (19)$$

Where R X is average shadowing system, n is path-loss component and c0 assumed -41.42dBm, E\_b^0 is energy per bit, found to be 1.82e-19(W) for a specified BER of 5e-5,

$$\frac{E_b^0}{N_0} = 7.6 \quad (20)$$

Fig(6) shows, for any modulation schemes, to achieve a higher data rate, the transmitter will require more power.

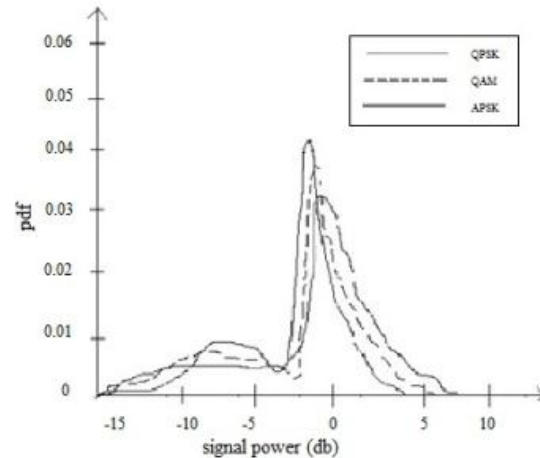


Fig.6Ultrawideband OFDM transceiver

## 10 Proposed system

### 10.1System Parameters

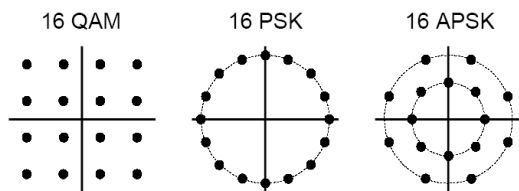
To transmit information, MB-UWB system uses convolution coding and puncturing to achieve a rate of 2/3, followed by OFDM modulation with M = 128 subcarriers. Fig.1 shows the proposed system model using M-APSK Modulation System transmitter and receiver. The input signal is assumed to be scrambled and coded. The encoder encodes the scrambled input signal. M-APSK mapping sets the constellation points for the encoded symbols, to find error detection and correction. The signal is then passed through a serial-to-parallel converter to separate the diversity branches. Each branch is separately demodulated using FFT algorithm. 128-

point IFFT is used at the transmitter. Similar to other OFDM systems, a cyclic prefix (CP) is added after the IFFT at the transmitter and discarded from the received signals before the FFT in each branch eliminates inter-symbol interference and inter-channel interference in all branches. At the receiver, the diversity branches are combined using equal gain combining followed by constellation de-mapping and decoding.

### 10.2 System Performance

To analyse the performance of the M-APSK modulation, a complete simulation of the system over the channel models described in the IEEE 802.15.3a UWB channel modeling report [7] is done. Here, the simulation results of CM1, CM2, CM3 and CM4 channels at extreme fading conditions are presented. Fig. 3 (a) to (d) shows the results over the CM1 to CM4 channel under log normal fading conditions. In this figure, the bit error rate is plotted versus the signal-to-noise ratio for all the channel models. The simulation results shows that the M-APSK system performance is stable for different channel model and achieves a BER nearly 10<sup>-6</sup> for SNR up to 10dB. The performance of M-APSK is better in additive white Gaussian noise (AWGN) channel .

### 10.3 Power Consumption



16 QAM has the largest distance between points, but requires very linear amplification. 16PSK has less stringent linearity requirements, but has less spacing between constellation points, and is therefore more affected by noise. M-ary schemes are more bandwidth efficient, but more susceptible to noise. MPSK and QAM are bandwidth efficient but not power efficient. M-APSK has optimum distance between points and variation in amplitude, which requires less power and minimum interference. Generally 'A' represents peak value of sinusoidal carrier. In the standard 1 ohm load register, the power dissipated will be,  $P = \frac{1}{2} A^2$ .

### 10.4 Channel Parameters

The IEEE 802.15.3a UWB channel parameters that is used for the simulation is given below in Table 2.

Table 2:- IEEE 802.15.3a UWB channel parameters

Model Parameters	CM1	CM2	CM3	CM4
$\Lambda$ [1/nsec] (cluster arrival rate)	0.0233	0.4	0.0667	0.0667
$\lambda$ [1/nsec] (ray arrival rate)	2.5	0.5	2.1	2.1
$\Gamma$ (cluster decay factor)	7.1	5.5	14.00	24.00
$\gamma$ (ray decay factor)	4.3	6.7	7.9	12
$\sigma_1$ [dB] (stand. dev. of cluster lognormal fading term in dB)	3.5	3.5	3.5	3.5
$\sigma_2$ [dB] (stand. dev. of ray lognormal fading term in dB)	3.4	3.4	3.4	3.4

### Channel Characteristics

	CM1	CM2	CM3	CM4
Mean excess delay	5.05ns	10.38ns	14.18ns	-
RMS delay spread	5.28ns	8.03ns	14.28ns	25ns
Distance	0-4m	0-4m	4-10m	10m
LOS/NLOS	LOS	NLOS	NLOS	NLOS

### 10.5 Simulation Results

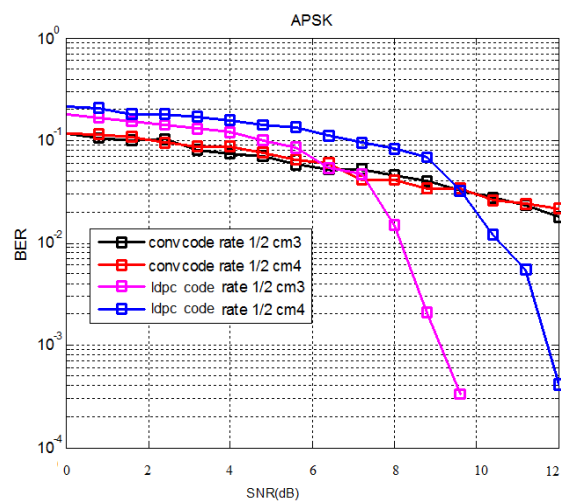


Fig: 10(a). LDPC and Convolutional codes with code rate 1/2 is compared in cm3 and cm4

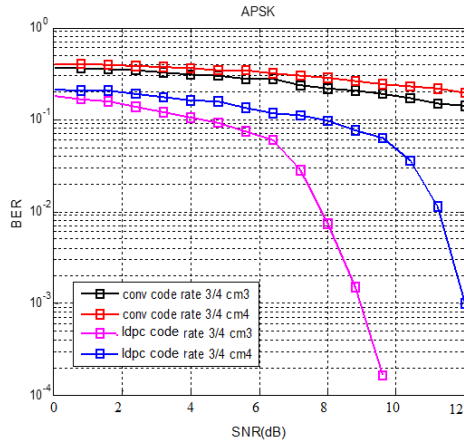


Fig:10(b). LDPC and Convolutional codes with code rate 3/4 is compared in cm3 and cm4

It can be observed from the above fig 4.9 that for lower SNR values (<1.5dB) BER values of both convolution and LDPC coded systems are comparable and are almost equal to  $10^{-1}$ . But for higher SNR values, BER of LDPC coded system decreases rapidly compare to convolutional coded system. LDPC Code of cm3 attains BER value nearly equal to  $10^{-4}$  for a SNR value of 2.5dB while SNR value should be 3dB for cm4 to achieve same BER. At the same time even for 3dB of SNR, convolutional code for cm3 and cm4 can achieve only a BER of slightly less than  $10^{-1}$ . So it can be inferred from the fig 4.9 that BER performance of LDPC coded system is better compared to that of convolutional coded system. It can also be inferred that among LDPC coded systems transmission power requirement is less for cm3 compared to cm4.

Comparison of Different Modulation Schemes is shown in table below which proves APSK provides high data Rates.

Data rate (in Mb/s)	Modulation	Code rate (R)
53.3	QPSK	1/3
160	QPSK	1/2
200	QPSK	5/8
320	DCM	1/2
400	DCM	5/8
480	DCM	3/4
640	16-QAM	1/2
640	16-PSK	1/2
640	16-APSK	1/2
960	16-APSK	3/4

## 11 Conclusion

Wireless-USB has now been standardized to use the services of Multiband OFDM (ECMA-368) as the transport mechanism. ECMA-368 offers a robust wireless solution and low power wireless service in WPAN.

This paper has been proposed a Low power and high performance LDPC-Coded APSK-modulation scheme that can fit into the configuration of ECMA-368 standard. This alternative modulation scheme can increase the system throughput to 960 Mb/s with outputting constant modulated symbol power, which is of great benefit to the AGC and ADC, resulting in a successful link of 3 meters in multipath environments. Thereby an effective data rate of 480 Mb/s can be achieved with moderate packet loss, even offer a higher throughput for comparable propagation conditions.

To achieve data rate of more than 1Gbps MIMO technology can be used

## Acknowledgements

This work was supported by SRM University-Chennai.

## References

- [1] Zaishuang Liu, QiuliangXie, KewuPeng, and Zhixing Yang,, “APSK Constellation with Gray Mapping : A genetic algorithm approach,” in *IEEE communications letters*, vol. 15, no. 12, december 2011 , pp. 1–6.
- [2] Marco Baldi, Franco Chiaraluce Antonio de Angelis, RossanoMarchesani, SebastianoSchillaci “Performance of APSK modulation in wireless tactical scenarios for land mobile systems”,*IEEE Transactions on Information Theory* , vol.28, no.1, may 2011 pp. 55–67, 1982.
- [3] R. De Gaudenzi, A. Guillen i Fabregas, and A. Martinez, “Performance analysis of turbo-coded APSK modulations over nonlinear satellite [1] channels”, *IEEE Transactions on Wireless Communications*, vol.5, no.9,pp. 2396-2407, September 2006
- [4] Saberinia, E., Tang, J., Tewfik, A.H., and Parhi, K.K., “Pulsed-OFDM Modulation for Ultrawideband Communications,” *IEEE Transactions on vehicular Technology*, Feb 2009, Vol. 58, No.2, pp. 720-726.

- [5] M. Z. Win and R. A. Scholtz, "On the robustness of ultra-wide bandwidth signals in dense multipath environments," *IEEE Commun. Lett.*, Feb. 1998, vol. 2, no. 2, pp. 51–53.
- [6] Balakrishnan, A. Batra, and A. Dabak, "A multi-band OFDM system for UWB communication," in *Proc. IEEE Conf. Ultra Wideband Syst. Technol.*, Nov. 2003, pp. 354–358.
- [7] J. Foerster et al., Channel Modeling Sub-Committee Report Final. 802.15 work group official web site. [Online]. Available: <http://grouper.ieee.org/groups/802/15/pub/2003/May03/>
- [8] L. Yang and G. B. Giannakis, "Ultra-wideband communications: an idea whose time has come," *IEEE Signal Processing Magazine*, vol. 21, no. 6, pp. 26–54, Nov 2004.
- [9] Omid Abedi; John Nielsen: "UWB Data rate and Channel Capacity in Modulation Schemes" , " *IEEE Trans. Commun*, Apr. 2000 vol. 48, no. 4, pp.1809–1826.
- [10] Jon Hamkins, Pasadena, "Performance of Low-Density Parity-Check Coded" *IEEE Trans. Commun*, Apr. 2010 vol. 18, no. 4, pp.1–14.
- [11] Design of a multiband OFDM system for realistic UWB channel environments," *IEEE Trans. Microwave Theory Techniques*", vol. 52, no. 9, pp. 2123–2138, Sept. 2004.
- [12] A. Batra et al., "Multiband OFDM physical layer specification," *WiMedia Alliance*, Release 1.5, August 2009.
- [13] J. Foerster et al., "Channel modeling sub-committee report final," IEEE P802.15-02/490r1-SG3a, Feb. 2003.
- [14] WiMediaAlliance <http://www.wimedia.org/en/index.asp>
- [15] ECMA-368, □High rate ultra wideband PHY and MAC standard, 1st Edition, December 2007.
- [16] ECMA-368, □High rate ultra wideband PHY and MAC standard, 3<sup>rd</sup> Edition, December 2008, also maintained as ISO/IEC 26907
- [17] USB-IF. Certified Wireless USB. <http://www.usb.org/developers/wusb/>
- [18] MBOA standard "MultiBand OFDM Physical Layer Proposal for IEEE 802.15.3a," September 2004, [http://www.wimedia.org/imwp/idms/popups/pop\\_download.asp?ContentID=6516](http://www.wimedia.org/imwp/idms/popups/pop_download.asp?ContentID=6516)
- [19] Runfeng Yang, Jianyong Bian, Cailian Zhu" Fixed Point Dual Circular 32-QAM Performance for Wireless USB" *IEEE Transactions on Wireless Communications*, vol.5, no.9, pp. 2396–2407, September 2011

### Authors' information

**C T Manimegalai** received the Bachelor of Engineering degree in Electronics and Communication Engineering from Bharathidasan University, Tamilnadu, India, in 1996. She received the Master of Engineering degree in Applied Electronics from Madurai Kamraj University, India in 1998. She has been working as Assistant Professor with SRM University, Chennai, India. She is pursuing PhD in the Department of Electronics and Communication Engineering, SRM University, Chennai, India. Her research interests are Ultra-Wideband, wireless sensor networks, image processing and MIMO-OFDM systems



**R Kumar** received the Bachelor's degree in Electronics and Communication Engineering from Bharathidasan University, Tamilnadu, India, in 1989, the Master of Science in 1993 from BITS Pilani and PhD degree from SRM University, Chennai in 2009. He is working as a Professor in the department of Electronics and Communication Engineering, SRM University, Chennai, India. He has 15 publications in Indian and International journals. He is currently guiding 6 PhD students. His areas of interest include spread spectrum techniques, wireless communication, cognitive radio, wireless sensor networks and MIMO-OFDM systems.

